Tellus (2003), 55B, 83–93
Printed in UK. All rights reserved

TELLUS
ISSN 0280–6509

Interannual variability of atmospheric CO_2 in the Mediterranean: measurements at the island of Lampedusa

By P. CHAMARD[1], F. THIERY[1], A. DI SARRA[1]*, L. CIATTAGLIA[2], L. DE SILVESTRI[1], P. GRIGIONI[1], F. MONTELEONE[3] and S. PIACENTINO[3], [1]*Division of Global Environment and Climate, ENEA,00060 S. Maria di Galeria, Rome, Italy;* [2]*Institute of Atmospheric Sciences and Climate, CNR, 00133 Rome, Italy;* [3]*Division of Global Environment and Climate, ENEA, 90141 Palermo, Italy*

(Manuscript received 3 January 2002; in final form 27 November 2002)

ABSTRACT

The atmospheric concentration of carbon dioxide and other greenhouse gases has been measured weekly since 1992 at the island of Lampedusa, in the Mediterranean sea. Lampedusa is a small island located approximately 100 km east of Tunisia, and 250 km south of Sicily. The 10-yr CO_2 data set has been analysed to quantify trends, and characterize semi-annual, annual and inter-annual variability. The data show an average trend of $+1.7$ ppmv yr^{-1}; the average annual cycle has an amplitude of about 9 ppmv. In the period of investigation the annual growth rate varies between 0.5 and 4.5 ppmv yr^{-1}, and the amplitude of the annual cycle between 7 and 11 ppmv yr^{-1}. By comparing the observed growth rate with recent estimates of carbon dioxide emissions, it is calculated that 58–61% of the emitted CO_2 remains in the atmosphere. The CO_2 growth rate appears to be related to large-scale dynamic phenomena, primarily El Niño/Southern Oscillation (ENSO). An evident signature of the 1997–98 El Niño is apparent in the CO_2 record, and corresponds to a weakening of the exchange with the biosphere. A high correlation between the global average temperature and the 12-month average carbon dioxide growth rate is also found. Wind direction displays a significant inter-annual variability throughout the measurement period, possibly influencing the observed evolution of the CO_2 concentration.

1. Introduction

Ice core studies have shown that the atmospheric carbon dioxide concentration has varied roughly between 180 and 290 ppmv throughout the last four glacial cycles (e.g. Petit et al., 1999), has remained at approximately 280 ppmv during the last interglacial period, and has dramatically increased since the industrial revolution. The atmospheric CO_2 concentration has been monitored at a few sites during the last 50 yr; new measurement stations have been progressively added, and high-quality observations are now available at many sites throughout the world. The present observations show that the carbon dioxide concentration has reached a value of about 365 ppmv, a concentration unprecedented in the last 400 000 yr; an increase by more than 25% with respect to the pre-industrial period has thus occurred. This increase, and its possible influence on the Earth's climate, has prompted the need for high-quality accurate measurements of the carbon dioxide concentration in the atmosphere. Accurate surface measurements of atmospheric CO_2 are also used to constrain the global carbon budget (see e.g. Tans et al., 1990) and to identify carbon source and sink regions (e.g. Tans et al., 1989; Fan et al., 1998; Bousquet et al., 2000, and others).

Beside anthropogenic emissions, many natural phenomena influence the CO_2 concentration in the atmosphere. Global-scale processes, like El Niño/Southern

*Corresponding author.
e-mail: disarra@casaccia.enea.it

Oscillation (e.g. Bacastow, 1976), changes in global temperature (Keeling et al., 1995; Braswell et al., 1997), precipitation (Elliott et al., 1991, and others), ocean upwelling (Rayner et al., 1999) and others, appear to be related to the carbon dioxide behaviour. These relationships are believed to proceed through a variety of mechanisms, such as photosynthesis and respiration by the terrestrial vegetation, uptake and emission from oceanic waters, assimilation by marine micro-organisms, storage and release by terrestrial soils, etc. In the global carbon dioxide budget the tropical oceans seem to play a fundamental role, indicating that certain regions may intervene more efficiently than others in the CO_2 balance. Little is known of the role on the Mediterranean in the global carbon dioxide budget. The Mediterranean sea has several peculiar characteristics that make this basin unique: it is the only large closed basin worldwide, and is characterized by a complex oceanic and atmospheric circulation. The Mediterranean is an oligotrophic basin, and CO_2 exchange with the marine ecosystem is probably small; Mediterranean forests appear, however, to be an efficient CO_2 sink (see e.g. Valentini et al., 2000).

For a better understanding of the role of the Mediterranean, long-term accurate measurements of the atmospheric CO_2 concentration are crucial, mainly in the marine environment.

In this paper, CO_2 concentration measurements carried out at a remote island in the Mediterranean are described. The obtained data set is analysed in relation to large-scale global phenomena. Influences from El Niño/Southern Oscillation and the North Atlantic Oscillation are considered, as well as relationships with the global temperature, and possible changes in the atmospheric circulation.

2. Analytical methods

The island of Lampedusa (35.5°N, 12.6°E), the position of which is shown in Fig. 1, is relatively isolated in the Mediterranean sea, about 100 km East of Tunisia, and 200 km North of Libya. Lampedusa has a surface area of about 20 km^2, is rocky, and has poor vegetation. On the south-eastern part of the island there is a village with 4000 inhabitants. Limited influence from the local vegetation and emissions is expected. The island has been selected for greenhouse gas measurements as a representative site of the central Mediterranean region. In 1992 the National Agency for New Technologies, Energy and Environment of Italy (ENEA) started a greenhouse measurement program at Lampedusa. Since 8 May 1992, atmospheric air has been sampled on a weekly basis to determine the carbon dioxide, methane, and other greenhouse gas concentrations. In the period 1992–1996 air samples were collected from the top of the 20 m tall lighthouse at Capo Grecale, on a promontory on the North-Eastern edge of Lampedusa (sampling altitude of ∼65 m). In 1997 a Laboratory for Climatic

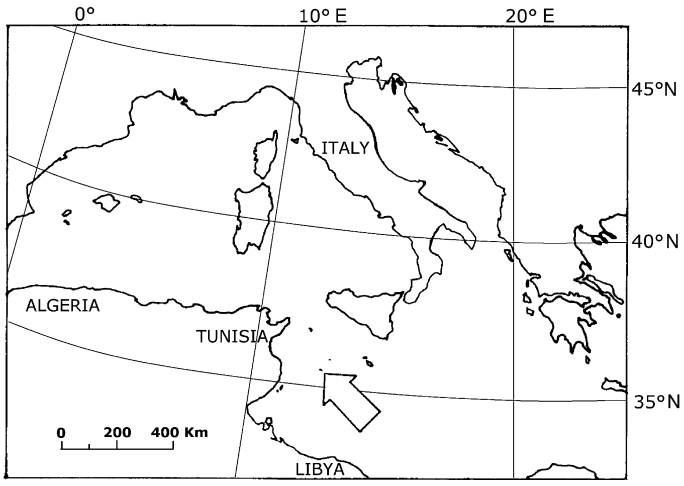

Fig. 1. Map of the central Mediterranean sea. The arrow indicates the position of the island of Lampedusa. Latitude N and longitude E are reported on the right and top axis, respectively.

Observations was established in a building close to Capo Grecale. At the laboratory total ozone, ultraviolet and visible radiation, and aerosol properties, besides greenhouse gases, are continuously measured (di Sarra et al., 2001a; b; 2002; Marenco et al., 2002). Since early 1997 atmospheric air has been sampled at an altitude of 2 m above the ground, approximately 45 m a.s.l. During the sampling procedure the atmospheric air is collected through a viton pipe by means of an oil free piston pump (Thomas 607CD22), flows through a magnesium perchlorate water vapour trap, and is pumped in a 2 L glass flask at a pressure of 3 bar. The flask valve has viton o-rings. Prior to the air sampling, flasks are emptied to about 5×10^{-2} mbar with a two-stage rotary vacuum pump (Edwards E2M1.5) to reduce the presence of resident impurities, and ambient air is flushed several times before collection. The carbon dioxide concentration is determined by means of an analyser composed of a set of electro-valves to select different air sources; a water vapour trap, constituted by a nafion dryer and a deep freezer that cools the air to approximately -70 °C; and a Siemens Ultramat 5E non-dispersive infrared (NDIR) analyser that measures the CO_2 relative concentration by determining the IR absorption of the gas sample through a cell 180 mm long. All the measuring gases and sampled air fluxes are regulated by a mass flow controller which maintains a stable and laminar flux at 300 cm^3 min^{-1} through the measuring cell.

The relative concentration is referred to an absolute scale through the following procedure: the gases from two cylinders, containing known amounts of CO_2, are used as working standards during the routine operations; their concentration is measured every 3 h by the same system, providing two extrema for the linear response interval of the analyser. Eight reference cylinders at known CO_2 concentration, provided by the Climate Monitoring and Diagnostic Laboratory (CMDL) at the National Oceanic and Atmospheric Administration (NOAA) and referred to the World Meteorological Organization scale, are used to calibrate the working standards once a week. Standards provided by the Central Calibration Laboratory of the Scripps Institute of Oceanography (SIO), La Jolla, California, were used before 2000. A cross check of the two sets of reference standards has shown that a very good agreement exists, and no correction to the measurements carried out prior to 2000 need be applied. The CO_2 concentration of the eight reference cylinders has been determined by comparison with primary standards, whose concentration was measured by an absolute method (Zhao et al., 1997).

The system, that allows the determination of the CO_2 concentration with an accuracy of about 0.1 ppmv, has been operational since 1992 at the Casaccia Laboratory (42.1°N, 12.3°E) of ENEA for the analysis of the weekly flask samples. In 1998 the system was installed at Lampedusa, where an aspiration pump allows the collection of atmospheric air from the top of a 10 m meteorological tower, and the continuous monitoring of carbon dioxide concentration. In 1991 and 1999 our group participated in round-robin tests carried out by the WMO to verify the consistency among different laboratories throughout the world. In each test, a set of three cylinders of air with unknown carbon dioxide concentrations were circulated and independently determined by the different laboratories. In the first round-robin experiment the average difference among the CO_2 concentrations measured at ENEA and those performed at the Scripps Institute of Oceanography was 0.03 ppmv (the reference standards were supplied by SIO at that time). In the second round-robin test, when standards from NOAA were used, the average difference between the ENEA and NOAA determinations was –0.14 ppmv.

In this paper the weekly flask measurements are presented and are analysed to identify signatures of large-scale phenomena.

3. Results and discussion

The time series of carbon dioxide measured at Lampedusa in the period May 1992 – March 2002 is shown in Fig. 2. Some general characteristics of the series may be outlined: a progressive increase is evident, with significant yearly variations. The large annual cycle, with a maximum in early spring, has an amplitude of approximately 10 ppmv. Relatively large variations, up to 4–5 ppmv, occur on a weekly basis, and are probably associated with different origins of the sampled air masses.

To identify the main periodicities that contribute to the cyclic behaviour of the CO_2 concentration a Fourier analysis has been carried out on the 499 available data. This analysis has confirmed the dominant role of the annual cycle; some role is played by the semi-annual cycle, while periods shorter than 6 months contributing negligibly. Thus, the CO_2 behaviour has been reconstructed by a least-squares fit with the equation

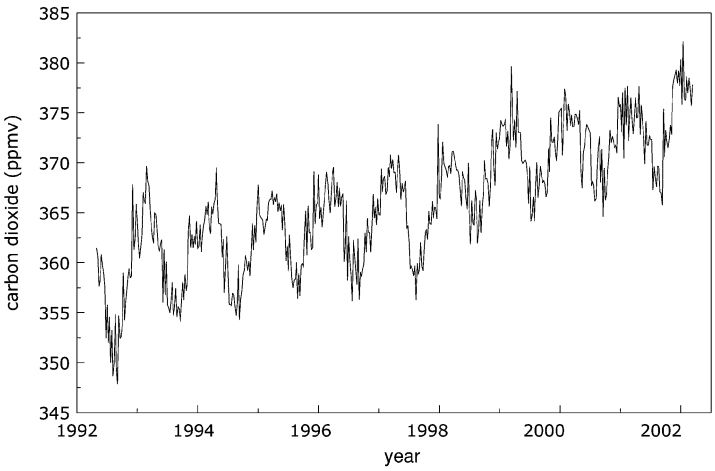

Fig. 2. Evolution of the weekly carbon dioxide concentration at Lampedusa. The ticks mark the beginning of each year.

$$y = c_1 + c_2 e^{\alpha m} + A \sin[2\pi(m + \phi_1)/T_1] + B \sin[2\pi(m + \phi_2)/T_2] \quad (1)$$

where y is the weekly carbon dioxide concentration, m is the week number (week 0 starts on 8 May 1992), α, c_1 and c_2 are constants, $T_1 = 26.07$ wk and $T_2 = 52.14$ wk are the semi-annual and annual periods, respectively, ϕ_1 and ϕ_2 are the semi-annual and annual phases (in wk), and A and B are the semi-annual and annual semi-amplitudes, respectively. Due to the limited length of the record, periods longer than 1 yr have not been included in the fit. The parameters obtained from the fit, calculated over the whole 1992–2002 time period, and assuming for c_1 (the CO_2 concentration at time $-\infty$) a value of 280 ppmv, are reported in Table 1.

The exponential growth term may be substituted by a linear term whose slope is given by αc_2; consequently, expression (1) has been substituted by the following equation:

$$y = a + bm + A \sin[2\pi(m + \phi_1)/T_1] + B \sin[2\pi(m + \phi_2)/T_2], \quad (2)$$

Table 1. *Parameters of the fit*

Parameter	Value
A	0.97 ppmv
B	4.35 ppmv
α	3.84×10^{-4} wk^{-1}
ϕ_1	5.52 wk
ϕ_2	23.10 wk

where a is a constant (corresponding to the CO_2 concentration at the beginning of the record) and b is a linear growth rate, GR, equal to 1.71 ppmv yr^{-1}. The annual cycle dominates the periodic behaviour, with an amplitude of about 9 ppmv (two times B). The semi-annual period has maxima in mid-May and mid-November.

As appears in Fig. 2, a large interannual variability is present. This variability is typical of carbon dioxide records, and is generally attributed to changes of emissions and/or changes of the amount of carbon held in biomass and soils, possibly affected by large-scale phenomena (see e.g. Conway et al., 1994, Keeling et al., 1995, and others). To study the interannual behaviour of CO_2, expression (2) has been fitted to the observations in 12 month periods, each period starting at the beginning of each month. In this way, a time series of the parameters of the fit are obtained. These parameters have been smoothed by calculating 12 month averages, to remove the variability induced by the variations of the fitting periods with respect to the dominating annual cycle. Figures 3 and 4 show the evolution of the 12-month averages of b (solid line), and of A and B, respectively. In the period 1993 to mid-1997 GR remains below 2 ppmv yr^{-1}. Years 1992 and 1993 are characterized by a low carbon dioxide growth rate (e.g. Lambert et al., 1995); this slow CO_2 increase has been related to the effects of the Pinatubo eruption in the Philippines in 1991.

A much faster increase of the CO_2 concentration takes place in the second half of 1997 and early 1998. A peak growth rate of about 4.5 ppmv yr^{-1} is reached

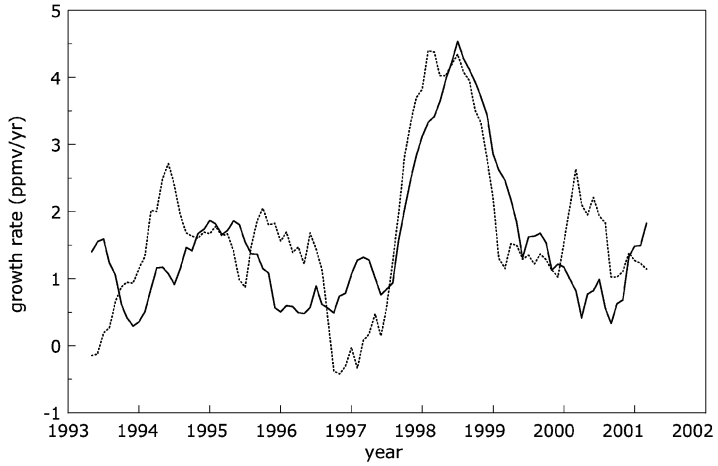

Fig. 3. Evolution of the 12-month averages of the CO_2 growth rate. The solid line is the growth rate calculated for the whole dataset, and the dotted line is the growth rate for the reduced dataset (see text). As in Fig. 2, the ticks mark the beginning of each year.

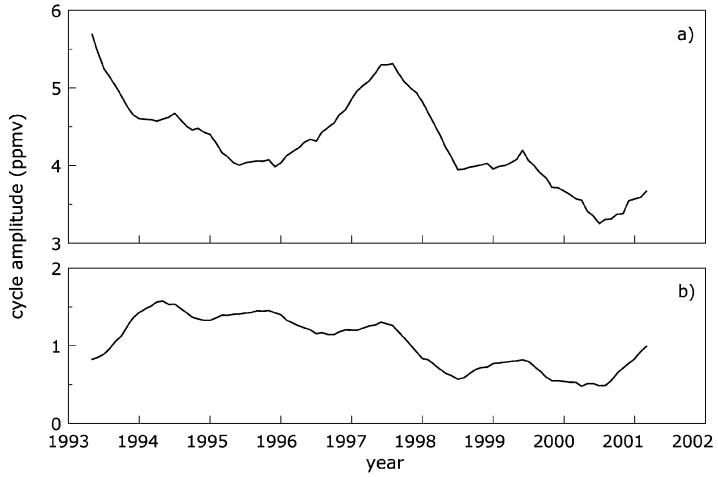

Fig. 4. Evolution of 12-month averages of (a) the annual and (b) semi-annual cycle amplitude. The ticks mark the beginning of each year.

in mid 1998. The CO_2 growth slows afterwards, returning to $\sim$1.5 ppmv yr^{-1} in late 1999. The peak growth rate of 4.5 ppmv yr^{-1} in mid 1998 appears as a high value, compared with the behaviour at other stations during other ENSO events (see e.g. Conway et al., 1994). The 1997–1998 ENSO event was, however, a very large one, and a more evident effect on the CO_2 growth rate may follow. A peak growth rate of about 4 ppmv yr^{-1} was reached in 1998 at Monte Cimone (44.2°N, Italy), a mountain station relatively close to Lampedusa (R. Santaguida, personal communication). It must be also emphasized that the peak GR is strongly affected by the way in which the data are smoothed. For instance, by applying a 12-month running mean to the GR of Fig. 3, the peak rate reduces to 3.9 ppmv yr^{-1}. We have investigated the possibility that the presence of CO_2 peaks in the weekly samples, attributable to the direct influence of sources or different origins of the sampled air masses, may affect the retrieved peak GR. To this purpose, the data set was divided into eight different classes, depending on the wind direction at the time of the air sampling (0° identifies

Table 2. *Amplitude of the annual cycle derived from data corresponding to the indicated wind sectors, and offset with respect to the annual cycle estimated from all the data*

Sector	Amplitude (ppmv)	Offset (ppmv)
0–45°	9.31	−0.06
45–90°	8.02	−0.16
90–135°	8.73	0.31
135–180°	8.54	−0.18
180–225°	7.87	−0.27
225–270°	9.98	−0.35
270–315°	10.32	0.44
315–360°	9.71	0.27
0–360°	9.03	0.00

winds from the north, 90° winds from the east). Then, the amplitude of the average annual cycle was calculated by fitting the detrended data with a two-harmonic (annual + semi-annual oscillation) sinusoidal function. The average annual cycle is somewhat different in each class. In particular, a constant offset with respect to the average annual cycle calculated for the whole dataset exists. The results of the analysis are reported in Table 2.

The data of all the four north-western sectors (winds originating from 225 to 45°) are characterized by a larger average annual amplitude; the sectors between 270 and 360° also display a positive constant bias of 0.2–0.4 ppmv, and are characterized by a somewhat higher CO_2 content. To identify the role of the data of the different classes on the overall results, the calculation of the growth rate was repeated on a reduced dataset, obtained by removing all the measurements carried out with winds originating between the north and west directions (winds from 270 to 360°). The GR for the reduced dataset is reported in Fig. 3: the elimination of the north-western data seems to produce a distinct effect on the results. The peak growth rate in 1998 remains at the same value, while differences appear in late 1993, throughout 1997 and early 2000. We can not exclude that a change in the sampling altitude that occurred in 1997 may also have affected the observations.

Changes of CO_2 emissions contribute to the observed growth rate behaviour. Marland et al. (2001) report estimates of the global carbon dioxide emissions from consumption and flaring of fossil fuels throughout the period 1751–1998. Emission estimates are also provided by the Energy Information Administration of the United States (available from the web site http://www.eia.doe.gov), which give also an estimate for 1999. We are not aware of estimates for 2000.

The total emissions throughout 1993–1998, as derived from Marland et al. (2001), is 38.5 Mton of carbon equivalent, which corresponds to an atmospheric CO_2 increase of 18.2 ppmv, based on a value of 5.12×10^{21} g for the dry mass of the atmosphere (Trenberth, 1981). The observed increase of the CO_2 concentration over the 1993–1998 period (calculated as the difference between the average CO_2 concentration of the period July 1998–June 1999, and that of the period July 1992–June 1993) is 10.5 ppmv. Under the assumption that the overall atmospheric CO_2 increase is due to anthropogenic emissions, it is calculated that about 57.7% of the emitted CO_2 remains airborne. This result may be compared with fractions of 53–59% previously derived by other studies (e.g. Peterson et al., 1986; Keeling et al., 1985; Thoning et al., 1989); however, obtained over different periods of time. A larger fraction, around 61%, is derived if the emission estimates performed by the U.S. Energy Information Administration, which are somewhat smaller than those reported by Marland et al. (2001), are used. As pointed out by Thoning et al. (1989), a large variability in the estimates of the fraction of carbon dioxide remaining in the atmosphere exists, depending on the considered time interval. This variability is only in a small part due to the interannual changes of the emissions, and mostly depends on the interannual variability of GR. The yearly changes of emission are expected to produce interannual changes of GR within ±0.1 ppmv yr^{-1}. This result does not depend on the emission dataset, since the interannual changes are similar in the two cases. The interannual change of atmospheric CO_2 attributable to emissions is much smaller than the observed GR variability, and we will assume in the following analyses that emissions play a minor role and the observed variations of b are dominated by other large-scale phenomena and by their changes.

Figures 3 and 4 shows that the changes of the growth rate are associated with significant variations of the annual and semi-annual cycle semi-amplitudes. The annual cycle amplitude has maxima of about 11 ppmv (twice the modulus of coefficient B) in 1993 and in mid 1997; values close to or smaller than 8 ppmv occur in 1995, and in 1998–2001. The semi-annual cycle amplitude is always smaller than 3 ppmv, and shows a maximum in early 1994. A large reduction of the annual and semi-annual amplitudes occurs in correspondence with the fast increase of the growth rate in 1998, indicating that changes of the CO_2 fluxes with

the vegetation may play a significant role in the determination of the behaviour of *b*. The evolution of the annual and semi-annual amplitudes show some similarities in the years 1997–2001, while they appear substantially different in the previous years.

Changes of the growth rate have been related to large-scale phenomena, like El Niño/Southern Oscillation (ENSO) (e.g. Bacastow, 1976, Conway et al., 1994, Keeling et al., 1995, and others). We have considered two large-scale processes, ENSO and the North Atlantic Oscillation, NAO, as indicators of important changes in the land–ocean–atmosphere system, capable to influence the atmospheric CO_2 balance. The evolution of ENSO is described by the Southern Oscillation Index, SOI; we have used in this study the index given by the normalized monthly mean sea level pressure difference between Tahiti and Darwin (Ropelewski and Jones, 1987). In a similar way, the North Atlantic Oscillation Index, NAOI, is defined as the normalized pressure difference between Gibraltar and South-Western Iceland (Reykjavik) (Jones et al., 1997). In Fig. 5 we have plotted 12-month averages of the Southern Oscillation index and of the North Atlantic Oscillation index, together with the 12-month average of *b*.

Linear cross correlation coefficients between SOI and the CO_2 growth rate were calculated for different time lags. Largest correlation (cross correlation coefficient of -0.54) is found for a time lag of 9 months on SOI; the value of the correlations coefficient is statistically significant at the 99% confidence level. Thoning et al. (1989) have found at Mauna Loa (19.5°N) a similar correlation, with a 5 month lag. Conway et al. (1994), analyzing data from the NOAA/CMDL global air sampling network, found an increase of the time lag with latitude. The 9 month lag for Lampedusa is one of the largest recorded values. As pointed out by Gaudry et al. (1991) and by Elliott et al. (1991), for each El Niño event the CO_2 growth rate shows a somewhat different behaviour. The lag producing the largest correlation between GR and SOI is somewhat shorter, 8 months, if the reduced dataset (i.e. only measurements obtained with winds from southern and eastern sectors) is used.

Anomalies of the Southern Oscillation Index are associated with sea level pressure, temperature, precipitation (see e.g. Elliott et al., 1991; Trenberth and Caron, 2000; and others), ocean upwelling (e.g. Rayner et al., 1999) and wind (Bacastow, 1976) anomalies, and modifications of their distributions. These anomalies may in different ways affect the CO_2 exchange among the atmosphere, and the terrestrial and marine ecosystems. During an El Niño warm event upwelling in the Eastern Pacific ocean is suppressed. Consequently, the CO_2 export to the atmosphere in the equatorial ocean, usually largely controlled by the upwelling of deep water, supersaturated in carbon dioxide, reduces. The upwelling suppression, moreover, produces a decrease of nutrients, also more abundant in the deep water, in the upper ocean layer. The reduction of nutrients induces a decrease of micro-organism concentration, and a less efficient carbon dioxide removal from the atmosphere. Temperature and precipitation affect CO_2 exchange mainly through terrestrial and

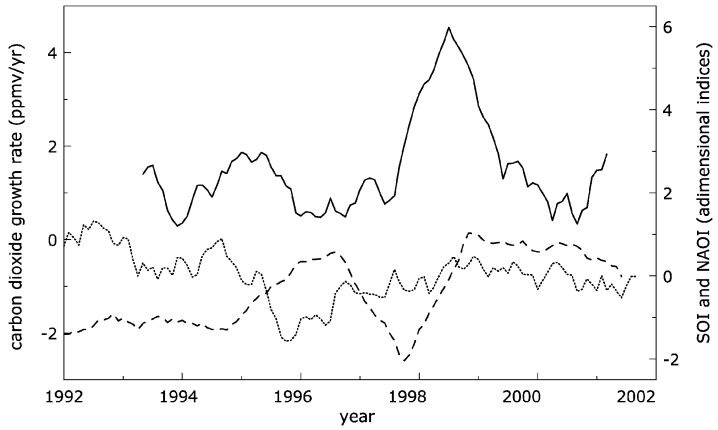

Fig. 5. Evolution of the 12-month averages of the CO_2 growth rate (solid line), Southern Oscillation index (dashed line) and North Atlantic Oscillation Index (dotted line). The two indices are nondimensional. The ticks mark the beginning of each year.

marine photosynthesis and respiration. Wind is also expected to play a role in the ocean–atmosphere CO_2 exchange, which depends on wind shear close to the ocean surface (Bacastow, 1976). The detailed knowledge of some of the basic processes is still incomplete. Moreover, other phenomena may play a role, and a quantitative understanding of the relationship between atmospheric CO_2 and El Niño is still problematic.

The CO_2 behaviour at Lampedusa appears dominated by the effect of the very large 1997/98 El Niño event. Consequently, the correlated behaviour between GR and SOI is particularly evident for the 1997/98 period. Also the annual and semi-annual amplitudes show a marked dependence. These amplitudes, which may be taken as indicators of exchange between the terrestrial vegetation and the atmosphere, distinctly decrease as GR increases, and show a recovery, more evident for the semi-annual amplitude, during the descending phase of *b* taking place in the time period between mid-1998 and mid-1999. Thus, the faster growth of the carbon dioxide seems to correspond to a slower uptake by the biosphere.

A linear relationship between the CO_2 growth rate and SOI lagged by 9 months in the period 1997–2000 has been used to derive an empirical carbon dioxide growth rate, GR_{SO}, dependent only on SOI. We calculated the difference between the observed GR and the empirical one estimated from SOI (GR_{SO}), and used this difference to calculate the cross correlation coefficient with the NAOI, also in this case for different time lags between the two datasets. The largest correlation (cross correlation coefficient of -0.24) between the NAOI and the CO_2 growth rate residuals is found for a NAOI time lag of 16 months. The series, as is also the case for the correlation with SOI, are negatively correlated. Bates (2001) has shown that anomalies of sea surface temperature, oceanic mixed layer depth, primary production and surface seawater total CO_2 in the North Atlantic subtropical gyre are correlated to NAO. The interannual variability of these parameters may in principle affect the oceanic CO_2 fluxes, and contribute to the modulation of the atmospheric CO_2 growth rate. NAOI is negative in the period mid-1995–1997; in the same interval, a decline of GR is observed. The maximum correlation is found when the NAOI is lagged by 16 months; in this case the NAOI decrease is associated with an increase of the residual of the CO_2 GR. It must be emphasized, however, that throughout the period of investigation the NAOI is significantly different from zero only in late 1995 – early 1996, and a single event appears not sufficient to derive a convincing conclusion. A longer time interval is needed to address this topic.

An important parameter descriptive of large-scale processes is the global average temperature. Temperature may affect CO_2 exchange through different mechanisms. For instance, photosynthetic processes are strongly dependent on temperature, as well as on water availability (see e.g. Keeling et al., 1995). Oceanic upwelling, with consequent transport of nutrients to the surface and increase of CO_2 absorbing organisms, on one side, and emission of excess dissolved carbon dioxide, on the other, are also significantly affected by temperature (see e.g. Falkowski et al., 2000). Temperature also controls soil carbon dynamics. As shown by Trumbore et al. (1996), carbon turnover time in the upper 20 cm of the soil decreases with temperature; as a consequence, soil may act as significant carbon dioxide source or sink, also depending on global temperature. Estimates of T_g, the temperature anomalies with respect to the period 1961–1990, were derived from Jones et al. (2001), and were compared with the CO_2 GR record at Lampedusa. The two curves are reported in Fig. 6.

The largest correlation, 0.89, is found for a 3-month lag in T_g. A large correlation between global temperature and CO_2 behaviour was found by several authors (e.g. Keeling et al., 1995; Braswell et al., 1997). Braswell et al. (1997) found a positive correlation between CO_2 growth rate and lagged temperature anomaly, when the lag is 0–7 months, with the largest correlation for a 3-month lag. The correlation is negative for about a 2 yr lag in the global temperature anomaly. Their results, which also make use of the normalized difference vegetation index, NDVI, show indications that global correlations are the result of the composition of individual responses of different ecosystems. It is interesting to note that in our case the correlation becomes negative for a 16-month lag in T_g, and the highest anti-correlation is reached for a lag of about 24 months. Similarly, a peak positive correlation of about 0.47 between the CO_2 GR and the SOI lagged by 28 months exists. The understanding of the relationships between the global temperature, that is also affected by phenomena like El Niño, and the CO_2 behaviour involves complex phenomena. A quantitative description of the dependence of CO_2 on temperature, as is the case for the dependence on ENSO and NAO, is still difficult to achieve.

Recently, Higuchi et al. (2002) have shown that shifts of the atmospheric circulation regime may produce interannual variations and quasi-decadal trends

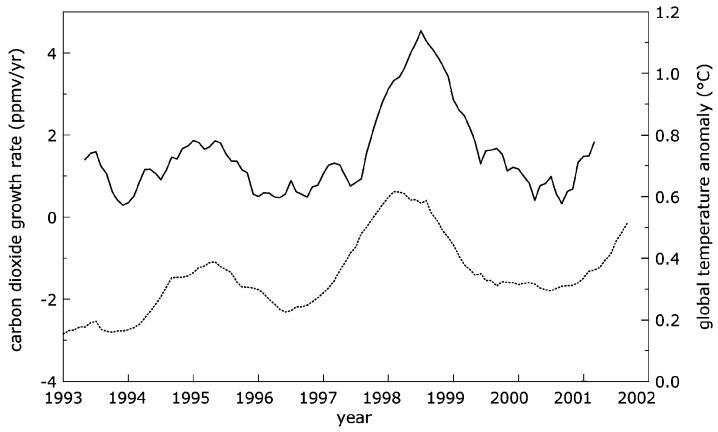

Fig. 6. Behaviour of the 12-month averages of the CO_2 growth rate (solid line), and of the global temperature anomaly from the 1961–1990 average (dotted line). The ticks mark the beginning of each year.

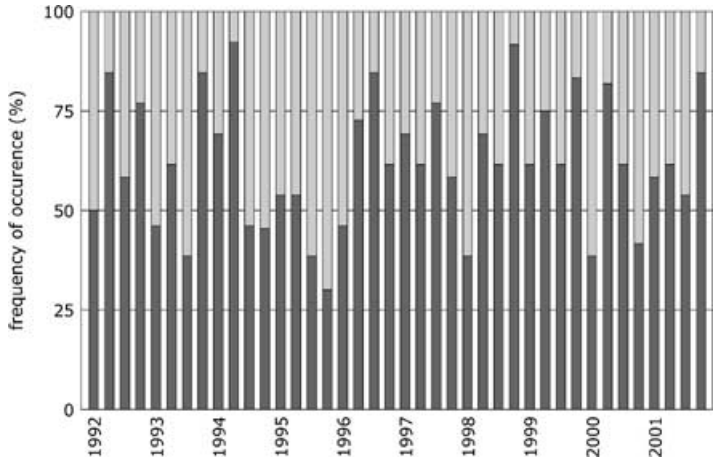

Fig. 7. Frequency of occurrence of wind direction in the north-western (winds from 225 to 45°, dark grey region) and south-eastern (winds from 45 to 225°, light grey region) sectors, in consecutive 3-month periods (period I, March–May; period II, June–August; period III, September–November; period IV, December–February). The labels of the year mark periods I.

of the CO_2 seasonal cycle amplitude; these variations and trends are of similar magnitude to the observed ones. We have previously shown that differences in the average annual cycle are associated with different wind directions, leading to the identification of two main directions, from 45 to 225° (south-eastern sectors), and from 225 to 45° (north-western sectors), that influence CO_2 behaviour. Figure 7 shows the percentage of occurrence of wind direction in the two main sectors, for 3-month periods, throughout the period of investigation. Seasonal and annual variations of the wind direction, possibly also related to large-scale phenomena, are present. No evident correlation of the frequency of occurrence of the wind direction with the CO_2 annual cycle amplitude, the growth rate or the difference ($GR - GR_{SO}$), is apparent. Although a dependency is not evident in our dataset, probably being masked by the stronger effect in El Niño, changes in the wind regime may contribute to the CO_2 observed inter-annual variability.

4. Conclusions

Accurate measurements of the atmospheric CO_2 concentration have been carried out on a weekly basis

on the island of Lampedusa, in the Mediterranean, since 1992. The island is relatively far from significant carbon dioxide sources, and may be considered representative of the central Mediterranean region.

The 10-yr CO_2 data set has been analysed with the aim of studying the interannual variability of the accumulation in the atmosphere, and of the semi-annual and annual components. Estimates of the annual growth rate expected from atmospheric emissions show that a fraction between 58 and 61% of the emitted carbon dioxide remained in the atmosphere. The annual average CO_2 growth rate has been calculated from the data set. The CO_2 growth rate interannual variability resulting from annual changes of emissions appears much smaller than the observed one. Thus, this variability must be attributed to different phenomena.

The CO_2 growth rate has been related to the Southern Oscillation index. The two quantities appear negatively correlated, and the largest correlation is found when the SOI is lagged by 9 months. A positive correlation is found for a SOI lag of about 2 yr. Analyses aimed at identifying possible relationships between the CO_2 growth rate and the North Atlantic oscillation require a longer interval of time; on the basis of the present dataset it is not possible to draw significant conclusions. The CO_2 growth rate has also been related to the global temperature, and a high correlation (0.89) for the temperature anomaly lagged by 3 months is found.

The wind direction shows seasonal and interannual variations in the observed period, and may contribute to the observed CO_2 behaviour.

All these results emphasize the role played by large-scale processes on the regulation of the carbon dioxide in the atmosphere, and on the carbon cycle.

5. Acknowledgements

This research has been supported by Ministry for Environment and by Ministry for Education, University and Research of Italy.

REFERENCES

Bacastow, R. B. 1976. Modulation of atmospheric carbon dioxide by the Southern Oscillation. *Nature* **261**, 116–118.

Bates, N. R. 2001. Interannual variability of oceanic CO_2 and biogeochemical properties in the Western North Atlantic subtropical gyre. *Deep Sea Res. II* **48**, 1507–1528.

Bousquet, P., Peylin, P., Ciais, P., Le Quéré, C., Friedlingstein, P. and Tans, P. P. 2000. Regional changes in carbon dioxide fluxes of land and oceans since 1980. *Science* **290**, 1342–1346.

Braswell, B. H., Schimel, D. S., Linder, E. and Moore, B. III. 1997. The response of global terrestrial ecosystems to interannual temperature variability. *Science* **278**, 870–872.

Conway, T. J., Tans, P. P., Waterman, L. S., Thoning, K., Kitzis, D. R., Masarie, K. A. and Zhang N. 1994. Evidence for interannual variability of the carbon cycle from the National Oceanic and Atmospheric Administration/Climate Monitoring and Diagnostics Laboratory Global Air Sampling Network. *J. Geophys. Res*. **99**, 22 831–22 855.

di Sarra, A., Cacciani, M., Campanelli, M., Chamard, P., Cornwall, C., DeLuisi, J., De Silvestri, L., Di Iorio, T., Disterhoft, P., Fiocco, G., Fuà, D., Grigioni, P., Junkermann, W., Marenco, F., Meloni, D., Monteleone, F. and Olivieri, B. 2001a. Radiation, ozone, and aerosol measurements at Lampedusa during the PAUR II Campaign. *IRS 2000: Current problems in atmospheric radiation* (ed. W. L. Smith and Yu. M. Timofeyev). A. Deepak Publishing, Hampton, Virginia, 1193–1196.

di Sarra, A., Di Iorio, T., Cacciani, M., Fiocco, G. and Fuà, D. 2001b. Saharan dust profiles measured by lidar from Lampedusa. *J. Geophys. Res*. **106**, 10 335–10 347.

di Sarra, A., Cacciani, M., Chamard, P., Cornwall, C., DeLuisi, J. J., Di Iorio, T., Disterhoft, P., Fiocco, G., Fuà, D. and Monteleone, F. 2002. Effects of desert dust and ozone on the ultraviolet irradiance at the Mediterranean island of Lampedusa during PAUR II. *J. Geophys. Res*. **107**, 8135, doi:10.1029/2000JD000139.

Elliott, W. P., Angell, J. K. and Thoning, K. W. 1991. Relation of atmospheric CO_2 to tropical sea and air temperatures and precipitation. *Tellus* **43B**, 144–155.

Falkowski, P., Scholes, R. J., Boyle, E., Canadell, J., Canfield, D., Elser, J., Gruber, N., Hibbard, K., Högberg, P., Linder, S., Mackenzie, F. T., Moore, B. III., Pedersen, T., Rosenthal, Y., Seitzinger, S., Smetacek, V. and Steffen, W. 2000. The global carbon cycle: A test of our knowledge of Earth as a system. *Science* **290**, 291–296.

Fan, S., Gloor, M., Mahlman, J., Pacala, S., Sarmiento, J., Takahashi, T. and Tans, P. P. 1998. A large terrestrial carbon sink in North America implied by atmospheric and oceanic carbon dioxide data and models. *Science* **282**, 442–446.

Gaudry, A., Monfray, P., Polian, G., Ardouin, B., Jegou, A. and Lambert G. 1991. Non-seasonal variations of atmospheric CO_2 concentrations at Amsterdam Island. *Tellus* **43B**, 136–143.

Higuchi, K., Murayama, S. and Taguchi, S. 2002. Quasi-decadal variation of the atmospheric CO_2 seasonal cycle due to atmospheric circulation changes: 1979–1998. *Geophys. Res. Lett*. **298**, 10.1029/2001GL013751.

Jones, P. D., Jónsson, T. and Wheeler, D. 1997. Extension to the North Atlantic Oscillation using early instrumental pressure observations from Gibraltar and South-West Iceland. *Int. J. Climatol*. **17**, 1433–1450.

Jones, P. D., Osborn, T. J., Briffa, K. R., Folland, C. K., Horton, E. B., Alexander, L. V., Parker, D. E. and Rayner, N. A. 2001. Adjusting for sampling density in grid box land and ocean surface temperature time series. *J. Geophys. Res*. **106**, 3371–3380.

Keeling, C. D., Whorf, T. P., Whalen, M. and van der Plicht, J. 1995. Interannual extremes in the rate of rise of atmospheric carbon dioxide since 1980. *Nature* **375**, 666–670.

Lambert, G., Monfray, P., Ardouin, B., Bonsang, G., Gaudry, A. and Kazan, V. 1995. Year-to-year changes in atmospheric CO_2. *Tellus* **47B**, 53–55.

Marenco, F., di Sarra, A. and DeLuisi, J. 2002. A methodology for determination of aerosol optical depth from the Brewer 300–320 nm ozone measurements. *Appl. Opt*. **41**, 1805–1814.

Marland, G., Boden, T. A. and Andres, R. J. 2001. Global, regional, and national CO_2 emissions. In: *Trends: A compendium of data on global change*, Carbon Dioxide Information Analysis Center, Oak Ridge National Laboratory, U.S. Department of Energy, Oak Ridge, Tenn., U.S.A.

Peterson, J. T., Komhyr, W. D., Waterman, L. S., Gammon, R. H., Thoning, K. W. and Conway, T. J. 1986. Atmospheric CO_2 variations at Barrow, Alaska, 1973–1982. *J. Atmos. Chem*. **4**, 491–510.

Petit, J. R., Jozuel, J., Raynaud, D., Barkov, N. I., Barnola, J.-M., Basile, I., Bender, M., Chappelaz, J., Davis, M., Delaygue, G., Delmotte, M., Kotlyakov, V. M., Legrand, M., Lypenkov, V. Y., Lorius, C., Pépin, L., Ritz, C., Saltzman, E. and Stievenard, M. 1999. Climate and atmospheric history of the past 420 000 years from the Vostok ice core, Antarctica. *Nature* **399**, 429–436.

Rayner, P. J., Law, R. M. and Dargaville, R. 1999. The relationship between tropical CO_2 fluxes and the El Niño-Southern Oscillation. *Geophys. Res. Lett*. **26**, 493–496.

Ropelewski, C. F. and Jones, P. D. 1987. An extension of the Tahiti-Darwin southern oscillation index. *Mon. Weather Rev*. **115**, 2161–2165.

Tans, P. P., Conway, T. J. and Nakazawa, T. 1989. Latitudinal distribution of the sources and sinks of atmospheric carbon dioxide derived from surface observations and an atmospheric transport model. *J. Geophys. Res.* **94**, 5151–5172.

Tans, P. P., Fung, I. Y. and Takahashi, T. 1990. Observational constraints on the global atmospheric CO_2 budget. *Science* **247**, 1431–1438.

Thoning, K. W., Tans, P. P. and Komhyr, W. D. 1989. Atmospheric carbon dioxide at Mauna Loa observatory. 2. Analysis of the NOAA GMCC data, 1974–1985. *J. Geophys. Res*. **94**, 8549–8565.

Trenberth, K. E. 1981. Seasonal variations in global sea level pressure and the total mass of the atmosphere. *J. Geophys. Res*. **86**, 5238–5246.

Trenberth, K. E. and Caron, J. M. 2000. The Southern Oscillation revisited: Sea level pressures, surface temperatures, and precipitation, *J. Clim*. **13**, 4358–4365.

Trumbore, S. E., Chadwick, O. A. and Amundson, R. 1996. Rapid exchange between soil carbon and atmospheric carbon dioxide driven by temperature change. *Science* **272**, 393–396.

Valentini, R., Matteucci, G., Dolman, A. J., Schulze, E.-D., Rebmann, C., Moors, E. J., Granier, A., Gross, P., Jensen, N. O., Pilegaard, K., Lindroth, A., Grelle, A., Bernhofer, C., Grunwald, T., Aubinet, M., Ceulemans, R., Kowalski, A. S., Vesala, T., Rannik, Ü., Berbigier, P., Loustau, D., Guðmundsson, J., Thorgeirsson, N., Ibrom, A., Morgenstern, K., Clement, R., Moncrieff, J., Montagnani, L., Minerbi, S. and Jarvis, P. G. 2000. Respiration as the main determinant of carbon balance in European forests. *Nature* **404**, 861–865.

Zhao, C. L., Tans, P. P. and Thoning, K. W. 1997. A high precision manometric system for absolute calibration of CO_2 in dry air. *J. Geophys. Res*. **102**, 5885–5894.